bioresources.com

Preparation and Characterization of Lignin-containing Nanofibrillated Cellulose

Tianqing Lan,[a,b] Haoran Liu,[a] Hui Li,[a] Yuyue Qin,[a] and Guojun Yue [c,*]

Lignin-containing nanofibrillated cellulose (LNFC) were prepared from p-toluenesulfonic acid (p-TsOH) pretreated sugarcane bagasse (SCB) using either formic acid (FA) or hydrochloric acid (HCl) and high-pressure homogenization. The composition, morphology, dispersity, crystallinity, particle size, thermal stability, and hydrophobicity of LNFC treated with FA (F- LNFC) and HCl (H- LNFC) were compared *via* electron microscopy, an X-ray diffractometer (XRD), a thermal gravimetric analyzer (TGA), a Fourier transform infrared spectroscope (FTIR), and water contact angle (WCA) analysis. The results of morphology and dispersity testing showed that LNFC with uniform dispersion were successfully prepared using a homogeneous pressure of 30 MPa and the F- LNFC particles were more stable in an aqueous solution. The crystallinity of the LNFC was well maintained after homogenization. The TGA, FTIR, and WCA data indicated that F-LNFC had better thermal stability and were more hydrophobic than H-LNFC because FA could esterify cellulose. Improved dispersity and thermal stability and increased crystallinity and hydrophobicity of cellulose nanofibrils would enhance the performance of nanocomposite materials.

Contact information: a: Faculty of Agriculture and Food, Kunming University of Science and Technology, 650500 Kunming, China; b: State Key Laboratory of Pulp and Paper Engineering, South China University of Technology, 510640 Guangzhou, China; c: SDIC Biotech Investment Co., Ltd., No. 147 Xizhimen Nanxiao Street, Xicheng district, 100034 Beijing, China;
*Corresponding author: yueguojun_sdic@163.com

INTRODUCTION

Cellulose nanofibrils (NFC) have attracted attention due to their non-toxicity and biodegradability (Zhu *et al*. 2016). In most studies on NFC, the expensive bleached wood pulp is commonly used as the starting material (Bian *et al*. 2017a; Xie *et al*. 2018). Lignin-containing cellulose nanofibrils (LNFC) have better thermal stability and are more hydrophobic than NFC because they contain lignin that is more hydrophobic and more difficult to pyrolyze than cellulose and hemicellulose (Poletto *et al*. 2012; Rojo *et al*. 2015). Furthermore, non-bleached lignocellulose can be adopted as the raw material for the preparation of LNFC, which simplifies preparation and reduces cost (Rojo *et al*. 2015). Thus, LNFC should be thoroughly studied. Wood is the raw material typically used for LNFC preparation, but excessive logging damages the environment. Therefore, sugarcane bagasse, an industrial cellulose-containing by-product with abundant reserves, is a potential alternative raw material for the preparation of LNFC.

p-Toluenesulfonic acid (p-TsOH) pretreatment is a novel lignocellulose treatment method that can remove 85% to 90% of lignin after 20 min of treatment at 80 °C (Bian *et al*. 2017a; Chen *et al*. 2017). This pretreatment causes little damage to cellulose, so the

bioresources.com

crystallinity and the proportion of cellulose are higher than most other treatment methods (Bian *et al*. 2017a). Furthermore, p-TsOH can be completely recycled as organic acid (Yang *et al*. 2019), which is environmentally friendly. Therefore, lignocellulose treated with p-TsOH can be regarded as a promising starting material for the preparation of cellulose nanofibrils.

This study investigated the feasibility of preparing LNFC using sugarcane bagasse (SCB) treated with p-TsOH as the starting material and applying formic acid (FA) or HCl treatment (the most common organic and inorganic acid treatment methods) and high-pressure homogenization. The composition, morphology, crystallinity, dispersibility, particle size, chemical group, thermal stability, and hydrophobicity of the two LNFC were determined and analyzed. This study provides references for high-value utilization of SCB and preparation of high-performance LNFC.

EXPERIMENTAL

Materials

Sugarcane bagasse samples were collected from Yunnan Xinping Nanen Sugar Paper Co., Ltd. (Yunnan, China). Formic acid (FA) (88 wt%), hydrochloric acid (HCl) (37%), and p-TsOH were purchased from Tianjin Wind Boat Chemical Reagent Technology Co., Ltd. (Tianjin, China). Carboxymethyl cellulose sodium (CMC) was purchased from Shanghai Aladdin Biochemical Technology Co., Ltd. (Shanghai, China). All chemicals were of analytical grade.

Methods

Preparation of cellulose nanofibrils

Sugarcane bagasse was ground and sieved with a 30-mesh screen and then pretreated with 65 wt% p-TsOH (ratio of 1:20) at 80 °C for 20 min (Bian *et al*. 2017a). The hydrolysis residue was washed to neutrality and marked as S-P. The S-P was treated with 88 wt% FA (ratio of 1:20) at 95 °C for 6 h and then washed to neutrality (Du *et al*. 2016a). The solid residue was marked as F-LCSR. The S-P was treated with 2 M HCl at 80 °C for 2 h, and the solid-liquid ratio of the S-P to HCl was 1:20 (w/v). Next, the solid residue was washed to neutrality and marked as H-LCSR. The F-LCSR and H-LCSR suspensions (0.2 wt%) were homogenized 20 times with a high-pressure homogenizer (GJJ-0.06/70MPa; Shanghai Noni Light Industrial Machinery Co., Ltd., Shanghai, China) at 30 MPa. After homogenization, the F-LCSR and H-LCSR suspensions were referred to as F-LNFC and H-LNFC, respectively.

Chemical composition

The chemical compositions including the cellulose, hemicellulose, and lignin contents of S-P, F-LCSR/F-LNFC, and H-LCSR/H-LNFC were determined according to the method from the National Renewable Energy Laboratory (Sluiter *et al*. 2012).

Scanning electron microscope (SEM) and transmission electron microscope (TEM)

The microstructures of S-P, F-LCSR, and H-LCSR were imaged by SEM (NoVananoSEM450; FEI Company, Portland, OR, USA). The photos of the samples were taken at 5 kV. The microstructures of F-LNFC and H-LNFC were imaged by TEM (HT7700; Hitachi, Tokyo, Japan). The imaging of the samples was performed at 100 kV.

bioresources.com

Particle size and zeta potential

  The particle size distribution and zeta potential of F-LNFC and H-LNFC suspensions were analyzed by a particle size and zeta potential analyzer (Zetasizer Nano ZS90; Malvern Instruments Limited, Malvern, England).

X-ray diffractometer (XRD)

  The samples of S-P, F-LCSR, H-LCSR, F-LNFC, and H-LNFC were analyzed by XRD (D/Max 2200; Rigaku, Tokyo, Japan) with Cu-Kα radiation ($\lambda = 1.54$ Å). The samples were scanned from 5° to 90° with a step size of 0.02°. The crystallinity index (CrI) was calculated with Eq. 1,

$$CrI = (I_{002} - I_{am}) \times 100\% / I_{002} \tag{1}$$

where I_{002} is the scattered intensity of diffraction (002) plane and I_{am} is the minimum intensity between the main peak and the secondary peak.

Thermal gravimetric analyzer (TGA)

  The thermal stabilities of S-P, F-LNFC, and H-LNFC were measured using a TGA (STA449 F3A00; Netzsch, Serb, Germany). Five mg of each sample was heated from ambient temperature to 600 °C in high purity nitrogen with a flow rate of 25 mL/min at a heating rate of 10 °C/min.

Fourier transform infrared (FTIR) spectroscopy

  The chemical compositions of S-P, LCSR, and LNFC were evaluated by means of an FTIR spectroscope (TENSOR27; Bruker Karlsruhe, Baden-Wurttemberg, Germany) at 400 cm^{-1} to 4000 cm^{-1} with a resolution of 4 cm^{-1}.

Hydrophobicity

  The preparation of CMC film and the nanocomposite films (CMC/F-LNFC and CMC/H-LNFC) was as follows: 100 mL of LNFC suspension with a solid content of 0.1 wt % was mixed with 0.6 g of glycerol and 2 g of CMC for 4 h at room temperature. The mixture was poured onto a glass plate (20 cm × 20 cm) and dried at 45 °C overnight. Then, the films were kept at 25 °C and 50% relative humidity for 2 d. The surface hydrophobicities of the films were measured using a contact angle meter (JY-82; Chengde Jinhe Instrument Manufacturing Co., Ltd., Hebei, China). The water contact angle (WCA) of the film was calculated as the average angle of at least five different positions.

Statistical analysis

  All experiments and assays were performed in triplicate. Origin 8.5 software was used for data analysis (OriginLab, Northampton, MA, USA). Data were analyzed using one-way analysis of variance and Student's t-test. The alpha level was $p < 0.05$.

RESULTS AND DISCUSSION

Composition

  Lignocellulose treated with p-TsOH often contains a high proportion of cellulose with a high crystallinity (Bian *et al*. 2017a). Therefore, it is a suitable raw material for the preparation of cellulose nanofibrils. In this study, F-LNFC and H-LNFC were prepared

bioresources.com

using p-TsOH-treated SCB. To investigate the characteristics of these two LNFC, the composition of lignocellulosic substrates was analyzed. In Table 1, the lignin, cellulose, and hemicellulose contents of S-P, F-LNFC, and H-LNFC are shown. It was found in Table 1 that, after FA and HCl treatment of S-P, the cellulose contents of F-LNFC and H-LNFC increased to 72.4% and 74.2% from 65.0%, the hemicellulose contents decreased to 16.9% and 18.5% from 21.3%, and the lignin contents were not significantly different ($p > 0.05$). The existence of lignin can make homogenization easier (Spence *et al.* 2010). In this study, the homogenization condition was 30 MPa, which is milder than most other studies (Du *et al.* 2016a).

Table 1. Composition of S-P, F-LCSR or F-LNFC, and H-LCSR or H-LNFC *

Samples	Cellulose (%)	Hemicellulose (%)	Lignin (%)
S-P	65.05 ± 0.07[a]	21.27 ± 0.33[a]	9.13 ± 0.11[a]
F-LCSR/F-LNFC	72.43 ± 0.62[b]	16.87 ± 0.24[b]	9.19 ± 0.17[a]
H-LCSR/H-LNFC	74.17 ± 0.62[c]	18.54 ± 0.65[c]	8.11 ± 0.46[a]

* Data with the different superscripts denote a statistically significant difference ($p < 0.05$). The values following ± are standard deviations. In this study, LNFC was produced using LCSR through homogenization. Therefore, the composition of LNFC was the same as that of LCSR.

Morphology and Dispersity

Figure 1a shows the microtopography of S-P, LCSR, and LNFC. The F-LCSR was smaller than the H-LCSR because formic acid degraded more cellulose and hemicellulose (Du *et al.* 2016a). The two LNFC exhibited a network structure, and H-LNFC had more agglomeration than F-LNRC. In addition, some lignin particles (black dots in the TEM photos of LNFC) were present (Bian *et al.* 2017b).
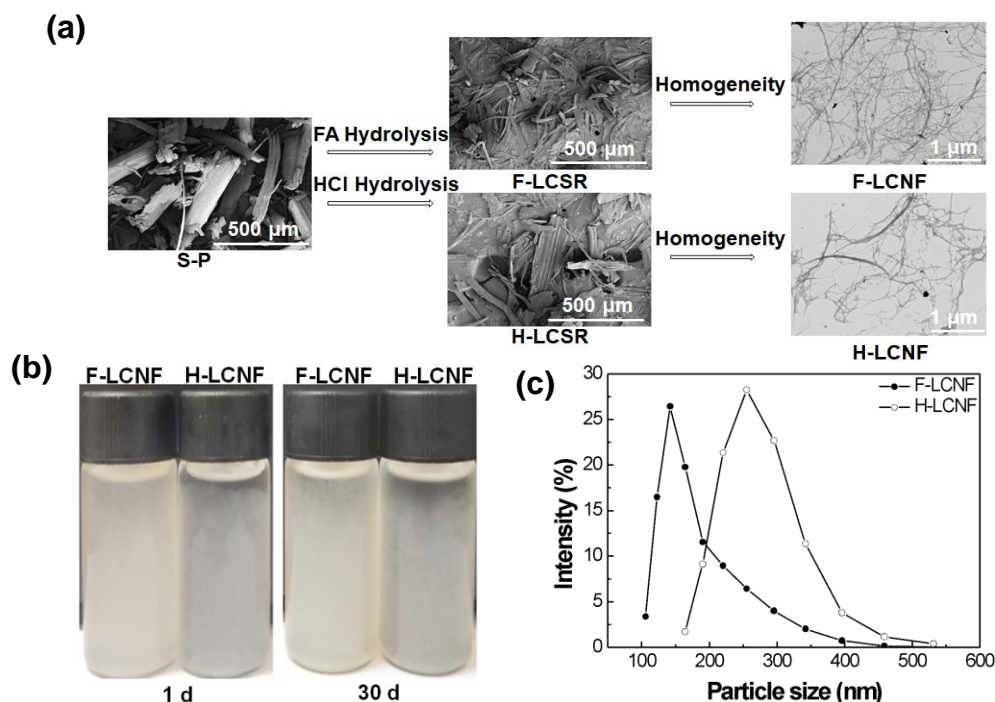

Fig. 1. SEM images of S-P and LCSR and TEM images of LNFC (a), LNFC suspensions after standing for 1 d and 30 d (b), and particle size distributions of LNFC (c)

bioresources.com

Dispersity is an important property of LNFC. To analyze the effect of size and morphology on the dispersibility of LNFC, photos of LNFC suspensions were taken after 1 d and 30 d of standing (Fig. 1b), and the particle size distributions of LNFC were measured (Fig. 1c). The LNFC suspensions did not have notable sedimentation after standing for 1 d and 30 d. The dispersity of F-LNFC was better than that of H-LNFC, which may have been due to its smaller size.

The dispersity of LNFC is influenced by surface charge and particle size. The average particle sizes and zeta potentials of LNFC are listed in Table 2. The zeta potential of F-LNFC was less negative than that of H-LNFC. The lower absolute value of zeta potential implies less electrostatic repulsion between the nanoparticles, which had a negative effect on the dispersion of LNFC particles (Liu *et al*. 2014). However, the small average size of F-LNFC (174.23 nm) relative to that of the H-LNFC (267.71 nm), was beneficial to the dispersion of nanofibrils (Jia *et al*. 2017). In other studies, the average particle sizes of cellulose nanocrystals ranged from 150 nm to 375 nm (Du *et al*. 2016b; Oun and Rhim 2017). In this study, F-LNFC had a relatively small average size and better dispersity. The smaller size could impact the uniform distribution of LNFC in suspension and composite materials (Oun and Rhim 2017).

Table 2. Average Particle Sizes of F-LNFC and H-LNFC*

Samples	F-LNFC	H-LNFC
Zeta Potential (mV)	-9.96 ± 1.75[a]	-29.63 ± 4.02[b]
Average Particle Size (nm)	174.23 ± 12.15[a]	267.71 ± 8.47[b]
* Data with the different superscripts denote a statistically significant difference ($p < 0.05$). The values following ± are standard deviations.		

Crystallinity

Because the crystallinity of cellulose nanofibrils can influence the properties of nanocellulose materials, the crystallinities of S-P, LCSR, and LNFC were measured. Figure 2 shows that after S-P was treated with FA and HCl, the crystallinities of F-LCSR and H-LCSR were 68.7% and 71.4%, respectively, which were higher than the 62.67% crystallinity of S-P. This was because FA and HCl removed some non-crystalline parts of the S-P substrate.
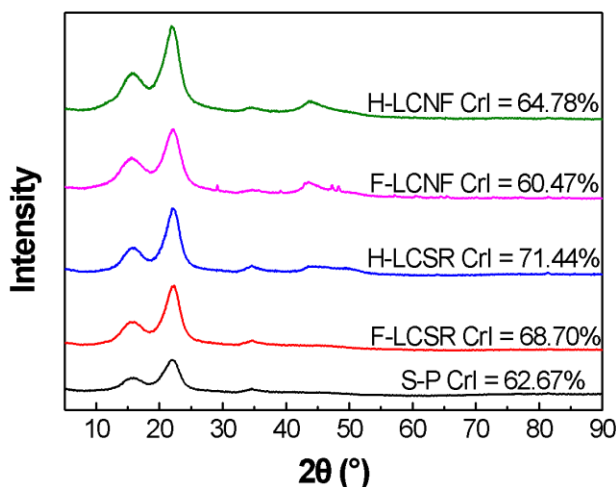

Fig. 2. The XRD spectrums of S-P, LCSR, and LNFC

bioresources.com

After homogenization, the crystallinities of F-LNFC and H-LNFC decreased to 60.5% and 64.8%, respectively, because high pressure homogenization can destroy the highly ordered crystalline region structure of the fiber by strong shear force (Saelee *et al.* 2016) and reduce the crystallinity (Hoeger *et al.* 2013).

After mild homogenization at 30 MPa, the crystallinities of F-LNFC and H-LNFCF decreased from 68.7% and 71.4% to 60.5% and 64.8%, respectively. This occurred because homogenization damaged the crystallization zone of cellulose (Saelee *et al.* 2016). However, the decrease in crystallinity observed in this study was lower than that of other studies due to using a relatively low homogenization pressure. The crystallinities of cellulose nanofibrils in previous studies ranged from 49.9% to 57.1% (Du *et al.* 2016a; Liu *et al.* 2016). Higher crystallinities enhance the mechanical properties of nanocomposites (Talbott *et al.* 1987).

Thermal Stability

To analyze the thermal stability of F-LNFC and H-LNFC, the initial pyrolysis temperature (T_{onest}) and maximum pyrolysis temperature (T_{max}) of S-P and LNFC were measured. The thermogravimetric (TG) and derivative thermogravimetric (DTG) curves of the samples are shown in Fig. 3. The T_{onest} and T_{max} of the samples are listed in Table 3. Figure 3 shows that there was slight weight loss at 100 °C. This was due to evaporation and the removal of water absorbed by the sample (Chirayil *et al.* 2014). Table 3 indicates that the initial and maximum pyrolysis temperatures of F-LNFC and H-LNFC were higher than those of S-P. Generally, the crystalline cellulose with high crystallinity had better thermal stability (Du *et al.* 2016b). In this study F-LNFC had lower crystallinity compared with H-LNFC and S-P; however, the thermal stability of F-LNFC was better than H-LNFC and S-P. This was because the thermal stability of cellulose nanoparticles was affected by not only crystallinity but also esterification of nanoparticles (Du *et al.* 2016b; Sun *et al.* 2016). Therefore, the better thermal stability of F-LNFC might be because that FA esterified S-P and made F-LNFC possess ester groups. It was reported in the literature (Sun *et al.* 2008), when the ester groups with better thermal stability replaced the hydroxyl groups with poor thermal stability on cellulose, the thermal stability of cellulose would be improved.
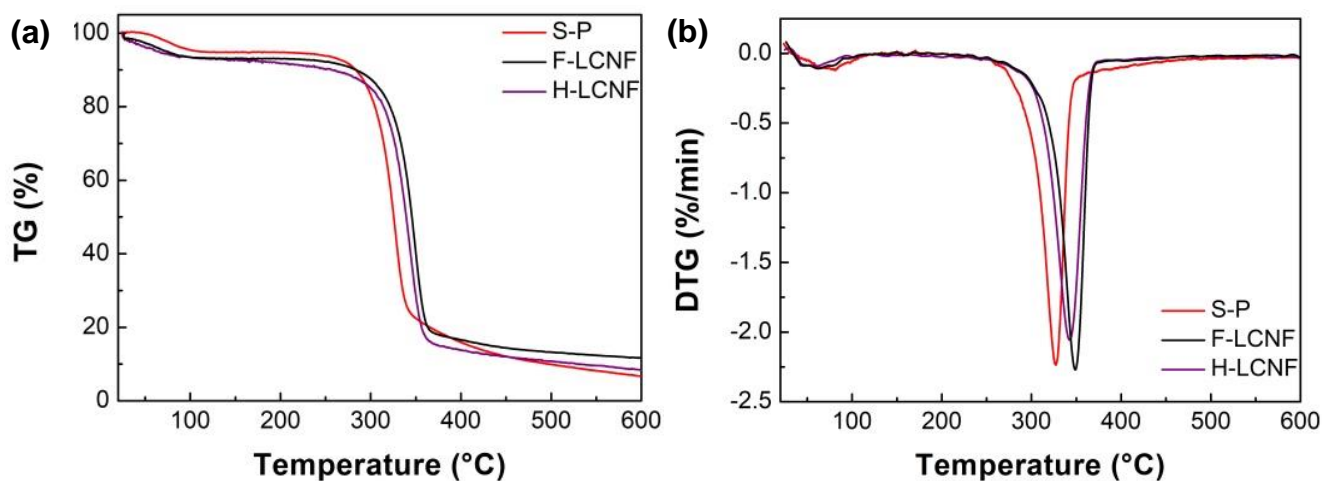

Fig. 3. The (a) TG and (b) DTG curves of S-P, F-LNFC, and H-LNFC

bioresources.com

The F-LNFC and H-LNFC in this study had higher thermal stability compared with the reported research. Jonoobim *et al*. (2015) summarized the thermal stability of more than a dozen NFC prepared with different raw materials and methods and found that the initial pyrolysis temperature and the maximum pyrolysis temperature ranged from 209 °C to 335 °C and 300 °C to 351 °C, respectively. The initial pyrolysis temperature and maximum pyrolysis temperature of F-LNFC were 309.09 °C and 350.00 °C, respectively, and these of H-LNFC were 300.00 °C and 341.67 °C, respectively. The phenyl in lignin was difficult to pyrolyze, which improved the thermal stability of LNFC (Poletto *et al*. 2012; Deepa *et al*. 2015). High thermal stability enhanced the thermoplasticity of the materials (Brinchi *et al*. 2013).

Table 3. Thermal Stabilities of the S-P, F-LNFC, and H-LNFC

Samples	T_{onset} (°C)	T_{max} (°C)
S-P	286.36	327.08
F-LNFC	309.09	350.00
H-LNFC	300.00	341.67

FTIR Analysis

The FTIR spectra of S-P and LNFC were determined (Fig. 4) to analyze the effect of FA and HCl treatment on the functional groups. Figure 4 shows that the F-LNFC spectrum showed a peak at 1720 cm^{-1} that represents the extension of ester group C=O in cellulose treated by FA (Sun *et al*. 2008). This was because when FA hydrolyzed S-P, the hydroxyl groups in the carboxyl groups of FA were combined with the hydrogen atoms in the hydroxyl groups of the cellulose and ester groups were formed (Sun *et al*. 2008).
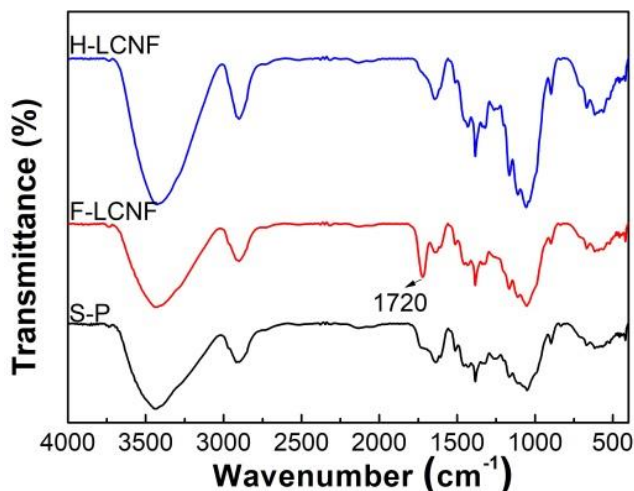

Fig. 4. The FTIR spectra of S-P, F-LNFC, and H-LNFC

Hydrophobicity

To analyze the hydrophobic properties of F-LNFC and H-LNFC, the WCA of CMC, F-LNFCF/CMC, and H-LNFC/CMC were measured using CMC as the blank carrier. The WCAs are listed in Table 4. The WCA of blank CMC film was 62.7°, which indicates that it was hydrophilic. After adding F-LNFC and H-LNFC, the WCAs of films increased to 102.7° and 111.2°, respectively ($p < 0.05$), which indicates that the films were more hydrophobic after adding LNFC. Lignin can affect the hydrophobicity of cellulose,

bioresources.com

and LNFC is generally more hydrophobic than NFC (Spence *et al*. 2010; Poletto *et al*. 2012). Table 4 also shows that the WCA of F-LNFC/CMC was larger than that of H-LFC/CMC (p < 0.05). The lignin contents of these two LNFC had no significant difference. This may have been due to F-LNFC containing more ester groups, which are hydrophobic (Scarica *et al*. 2018).

Table 4. Water Contact Angle of LNFC Films *

Samples	CMC	F-LNFC/CMC	H-LNFC/CMC
WCA (°)	62.74 ± 1.59[a]	111.18 ± 1.42[b]	102.7 ± 1.58[c]
* Data with the different superscripts denote a statistically significant difference (p < 0.05). The values following ± are standard deviations.			

CONCLUSIONS

1. The formic acid-treated lignin-containing nanofibrillated cellulose (F-LNFC) prepared from p-TsOH pretreated sugarcane bagasse (S-P) had better dispersity than the HCl-pretreated version (H-LNFC), which was attributed to the smaller particle size of the F-LNFC.

2. The LNFC in this study had higher crystallinity and better thermal stability than those reported in other studies.

3. The F-LNFC was more hydrophobic than the H-LNFC because formic acid esterified cellulose and formed more ester groups in the F-LNFC.

ACKNOWLEDGMENTS

REFERENCES CITED

Bian, H. Y., Chen, L. H., Gleisner, R., Dai, H. Q., and Zhu, J. Y. (2017a). "Producing wood-based nanomaterials by rapid fractionation of wood at 80 °C using a recyclable acid hydrotrope," *Green Chemistry* 19(14), 3370-3379. DOI: 10.1039/c7gc00669a

Bian, H. Y., Chen, L. H., Dai, H. Q., and Zhu, J. Y. (2017b). "Integrated production of lignin containing cellulose nanocrystals (LCNC) and nanofibrils (LCNF) using an easily recyclable di-carboxylic acid," *Carbohydrate Polymers* 167, 167-176. DOI: 10.1016/j.carbpol.2017.03.050

Brinchi, L., Cotana, F., Fortunati, E., and Kenny, J. M. (2013). "Production of nanocrystalline cellulose from lignocellulosic biomass: Technology and applications," *Carbohydrate Polymers* 94(1), 154-169. DOI: 10.1016/j.carbpol.2013.01.033

Chen, L. H., Dou, J. H., Ma, Q. L., Li, N., Wu, R. C., Bian, H. Y., Yelle, D. J., Vuorinen, T., Fu, S. Y., Pan, X. J., *et al*. (2017). "Rapid and near-complete dissolution of wood

lignin at ≤80 °C by a recyclable acid hydrotrope," *Science Advances* 3(9), 1-11. DOI: 10.1126/sciadv.1701735

Chirayil, C. J., Joy, J., Mathew, L., Mozetic, M., Koetz, J., and Thomas, S. (2014). "Isolation and characterization of cellulose nanofibrils from *Helicteres isora* plant," *Industrial Crops and Products* 59, 27-34. DOI: 10.1016/j.indcrop.2014.04.020

Deepa, B., Abraham, E., Cordeiro, N., Mozetic, M., Mathew, A. P., Oksman, K., Faria, M., Thomas, S., and Pothan, L. A. (2015). "Utilization of various lignocellulosic biomass for the production of nanocellulose: A comparative study," *Cellulose* 22(2), 1075-1090. DOI: 10.1007/s10570-015-0554-x

Du, H. S., Liu, C., Zhang, Y. D., Yu, G., Si, C. L., and Li, B. (2016a). "Preparation and characterization of functional cellulose nanofibrils via formic acid hydrolysis pretreatment and the followed high-pressure homogenization," *Industrial Crops and Products* 94, 736-745. DOI: 10.1016/j.indcrop.2016.09.059

Du, H. S., Liu, C., Mu, X. D., Gong, W. B., Lv, D., Hong, Y. M., Si, C. L., and Li, B. (2016b). "Preparation and characterization of thermally stable cellulose nanocrystals *via* a sustainable approach of $FeCl_3$-catalyzed formic acid hydrolysis," *Cellulose* 23(4), 2389-2407. DOI: 10.1007/s10570-016-0963-5

Hoeger, I. C., Nair, S. S., Ragauskas, A. J., Deng, Y. L., Rojas, O. J., and Zhu, J. Y. (2013). "Mechanical deconstruction of lignocellulose cell walls and their enzymatic saccharification," *Cellulose* 20(2), 807-818. DOI: 10.1007/s10570-013-9867-9

Jia, C., Chen, L. H., Shao, Z. Q., Agarwal, U. P., Hu, L. B., and Zhu, J. Y. (2017). "Using a fully recyclable dicarboxylic acid for producing dispersible and thermally stable cellulose nanomaterials from different cellulosic sources," *Cellulose* 24(6), 2483-2498. DOI: 10.1007/s10570-017-1277-y

Jonoobim, M., Oladi, R., Davoudpour, Y., Oksman, K., Durfresne, A., Hamzeh, Y., and Davoodi, R. (2015). "Different preparation methods and properties of nanostructured cellulose from various natural resources and residues: A review," *Cellulose* 22(2), 935-969. DOI: 10.1007/s10570-015-0551-0

Liu, Y. F., Wang, H. S., Yu, G., Yu, Q. X., Li, B., and Mu, X. D. (2014). "A novel approach for the preparation of nanocrystalline cellulose by using phosphotungstic acid," *Carbohydrate Polymers* 110, 415-422. DOI: 10.1016/j.carbpol.2014.04.040

Liu, C., Li, B., Du, H. S., Lv, D., Zhang, Y. D., Yu, G., Mu, X. D., and Peng, H. (2016). "Properties of nanocellulose isolated from corncob residue using sulfuric acid, formic acid, oxidative and mechanical methods," *Carbohydrate Polymers* 151, 716-724. DOI: 10.1016/j.carbpol.2016.06.025

Oun, A. A., and Rhim J.-W. (2017). "Characterization of carboxymethyl cellulose-based nanocomposite films reinforced with oxidized nanocellulose isolated using ammonium persulfate method," *Carbohydrate Polymers* 174, 484-492. DOI: 10.1016/j.carbpol.2017.06.121

Poletto, M., Zattera, A. J., Forte, M. M. C., and Santana, R. M. C. (2012). "Thermal decomposition of wood: Influence of wood components and cellulose crystallite size," *Bioresource Technology* 109, 148-153. DOI: 10.1016/j.biortech.2011.11.122

Rojo, E., Peresin, M. S., Sampson, W. W., Hoeger, I. C., Vartiainen, J., Laine, J., and Rojas, O. J. (2015). "Comprehensive elucidation of the effect of residual lignin on the physical, barrier, mechanical and surface properties of nanocellulose films," *Green Chemistry* 17(3), 1853-1866. DOI: 10.1039/c4gc02398f

Saelee, K., Yingkamhaeng, N., Nimchua, T., and Sukyai, P. (2016). "An environmentally friendly xylanase-assisted pretreatment for cellulose nanofibrils isolation from

sugarcane bagasse by high-pressure homogenization," *Industrial Crops and Products* 82, 149-160. DOI: 10.1016/j.indcrop.2015.11.064

Scarica, C., Suriano, R., Levi, M., Turri, S., and Griffini, G. (2018). "Lignin functionalized with succinic anhydride as building block for biobased thermosetting polyester coatings," *ACS Sustainable Chemistry & Engineering* 6(3), 3392-3401. DOI: 10.1021/acssuschemeng.7b03583

Sluiter, A., Hames, B., Ruiz, R., Scarlata, C., Sluiter, J., Templeton, D., and Crocker, D. (2012). *Determination of Structural Carbohydrates and Lignin in Biomass* (NREL/TP-510-42618), National Renewable Energy Laboratory, Golden, CO, USA.

Spence, K. L., Venditti, R. A., Rojas, O. J., Habibi, Y., and Pawlak, J. J. (2010). "The effect of chemical composition on microfibrillar cellulose films from wood pulps: Water interactions and physical properties for packaging applications," *Cellulose* 17(4), 835-848. DOI: 10.1007/s10570-010-9424-8

Sun, B., Yu, H. Y., Zhou, Y., Huang, Z., and Yao, J. M. (2016). "Single-step extraction of functionalized cellulose nanocrystal and polyvinyl chloride from industrial wallpaper wastes," *Industrial Crops and Products* 89, 66-77. DOI: 10.1016/j.indcrop.2016.04.040

Sun, Y., Lin, L., Deng, H. B., Li, J. Z., He, B. H., Sun, R. C., and Ouyang, P. K. (2008). "Structural changes of bamboo cellulose in formic acid," *BioResources* 3(2), 297-315. DOI: 10.15376/biores.3.2.297-315

Talbott, M. F., Springer, G. S., and Berglund, L. A. (1987). "The effects of crystallinity on the mechanical properties of PEEK polymer and graphite fiber reinforced PEEK," *Journal of Composite Materials* 21(11), 1056-1081. DOI: 10.1177/002199838702101104

Xie, H. X., Du, H. S., Yang, X. G., and Si, C. L. (2018). "Recent strategies in preparation of cellulose nanocrystals and cellulose nanofibrils derived from raw cellulose materials," *International Journal of Polymer Science* 2018, 1-25. DOI: 10.1155/2018/7923068

Yang, M. Y., Gao, X. F., Lan, M., Dou, Y., and Zhang, X. (2019). "Rapid fractionation of lignocellulosic biomass by p-TsOH pretreatment," *Energy & Fuels* 33(3), 2258-2264. DOI: 10.1021/acs.energyfuels.8b03770

Zhu, H., Luo, W., Ciesielski, P. N., Fang, Z., Zhu, J. Y., Henriksson, G., Himmer, M. E., and Hu, L. (2016). "Wood-derived materials for green electronics, biological devices, and energy applications," *Chemical Reviews* 116(16), 9305-9374. DOI: 10.1021/acs.chemrev.6b00225